American Mineralogist, Volume 70, pages 134–140, 1985

Scapolite: alkali atom configurations, antiphase domains, and compositional variations

C. Page Chamberlain, Janet A. Docka, Jeffrey E. Post, and Charles W. Burnham

Department of Geological Sciences
Harvard University, Cambridge, Massachusetts 02138

Abstract

Electrostatic energy calculations on an intermediate scapolite indicate that Na^+ should prefer to be adjacent to Cl^- anions and Ca^{2+} to be adjacent to CO_3^{2-} radicals. The calculations also indicate that short-range ordering of Na_4Cl and Ca_4CO_3 clusters is energetically favored and might give rise to antiphase domains.

Electrical neutrality considerations on the anion/radical site in scapolite suggest that the unusual compositional variations observed in the marialite–meionite series are the result of crystallographic constraints on the two possible independent exchange reactions in scapolite: $NaCl\overline{CaCO_3}$ and $NaSi\overline{CaAl}$. The compositions of naturally occurring scapolites may be explained in terms of the scapolite composition that represents local charge balance between Ca^{2+}, Na^+ cations and Cl^-, CO_3^{2-} anions.

Introduction

Scapolite can be regarded as a solid solution between marialite, $Na_4Al_3Si_9O_{24}Cl$, and meionite, $Ca_4Al_6Si_6O_{24}CO_3$. At compositions between these two end members scapolite is structurally complex. In this paper, we use electrostatic energy calculations and charge neutrality calculations to address three of these complexities: (1) the distribution of Na^+ and Ca^{2+} around Cl^- and CO_3^{2-} at intermediate scapolite compositions, (2) the origin of antiphase domains and, (3) the unusual trend of scapolite compositional variation.

Scapolite is a framework silicate consisting of two types of four-membered rings made up of AlO_4^{-5} and SiO_4^{-4} tetrahedra (Fig. 1; Levien and Papike, 1976; Papike and Zoltai, 1965). In one ring all tetrahedra point in the same direction, whereas in the other ring two tetrahedra point up and two point down (Fig. 1). These rings are arranged such as to outline continuous channels parallel to **c** that contain Na^+ and Ca^{2+}, and large cages that contain Cl^- and CO_3^{2-} (Fig. 1).

The inclusion of Cl^- and CO_3^{2-} within the scapolite framework permits three coupled substitutions: (1) the familiar $NaSi\overline{CaAl}$ as in feldspars, (2) $NaCl\overline{CaCO_3}$, and (3) $AlCl\overline{SiCO_3}$, which is a linear combination of the first two (see Thompson, 1982, for a description of the exchange vector notation). The composition space accessible to marialite-meionite scapolites is shown in Figure 2.

Configuration of Na^+ and Ca^{2+} within scapolite

Crystal structure refinements have been reported for Na-rich scapolites (Papike and Zoltai, 1965; Lin and Burley, 1973a), intermediate scapolites (Levien and Papike, 1976; Lin and Burley, 1975), and Ca-rich scapolites (Papike and Stephenson, 1966; Lin and Burley, 1973b). None of these studies have determined the relative distribution of Na^+ and Ca^{2+} around the Cl^- and CO_3^{2-} sites. They give, instead, positional parameters for a single undifferentiated (Na^+,Ca^{2+}) site, and they have further assumed that Na^+ is adjacent to Cl^- and Ca^{2+} is adjacent to CO_3^{2-} (Levien and Papike, 1976; Lin and Burley, 1975). We report here the results of electrostatic energy calculations on an intermediate scapolite that show that the most energetically favorable configuration of alkali cations within the scapolite structure bears out previous assumptions.

Calculations

Electrostatic energies were calculated using room temperature structural data (Levien and Papike, 1976) for an intermediate scapolite (atom ratio Ca/(Ca+Na) = 0.375 and Al/Si = 0.5), that is completely ordered with respect to Al^{3+} and Si^{4+} (Lin, 1975; Levien and Papike, 1976). Aluminum occupies T2 tetrahedra and silicon occupies T1 and T3 tetrahedra (Fig. 1). Sodium and calcium cations fill the large, oval-shaped channels shown in Figures 3 and 4 and surround the chlorine and carbonate anions situated on the $\bar{4}$-fold axis. This intermediate scapolite contains one Cl^-, one CO_3^{2-}, five Na^+, and three Ca^{2+} ions per unit cell. There are six distinguishable configurations of five Na^+ and three Ca^{2+} ions that can surround the one Cl^- and one CO_3^{2-} ion; we have investigated the electrostatic energies of all six.

0003–004X/85/0102–0134$02.00

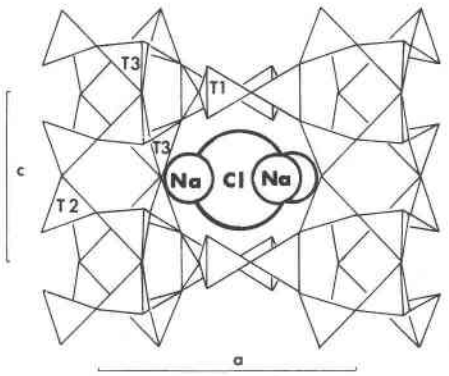

Fig. 1. The structure of marialite scapolite projected down a (modified from Levien and Papike, 1976).

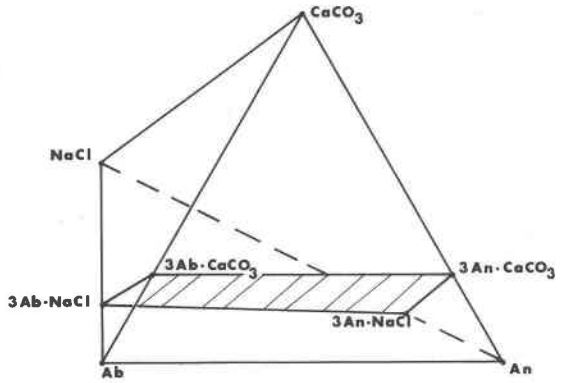

Fig. 2. Composition space for marialite–meionite scapolites. Shaded area is the theoretically possible plane for scapolite compositions.

Structure energies were calculated using the computer program WMIN (Busing, 1981). Short range (repulsive) energies for anion–cation and anion–anion interactions were approximated using Born's exponential form (Kittel, 1976, p. 88). The values for λ and ρ in the Born equation for the ion pairs (Table 1) were calculated using the modified electron gas (MEG) theory (Gordon and Kim, 1972), with the computer program LEMINPI (Muhlhausen and Gordon, 1981). Shell-stabilized Hartree Fock wave functions were used for O^{2-} and Cl^- in the MEG calculations, with shell radii of 1.01Å and 1.64Å, respectively. The charged shells approximate the potential surrounding the anion within a crystal. The use of stabilized functions is necessary for oxygen because the isolated O^{2-} ion is not stable. By changing the shell radii, it is possible to adjust the effective sizes of the Cl^- and O^{2-} (i.e., isotropic polarization). In practice a shell radius is used such that the shell charge (+1 for Cl, and +2 for O) divided by the shell radius equals the anion site potential (Muhlhausen and Gordon, 1981).

In order to calculate the energy for the six different configurations of Na^+ and Ca^{2+}, we have made several simplifying assumptions. First, because the CO_3^{2-} occupies a site having $\bar{4}$ symmetry, previous authors (Levien and Papike, 1976) argued that it must be positionally

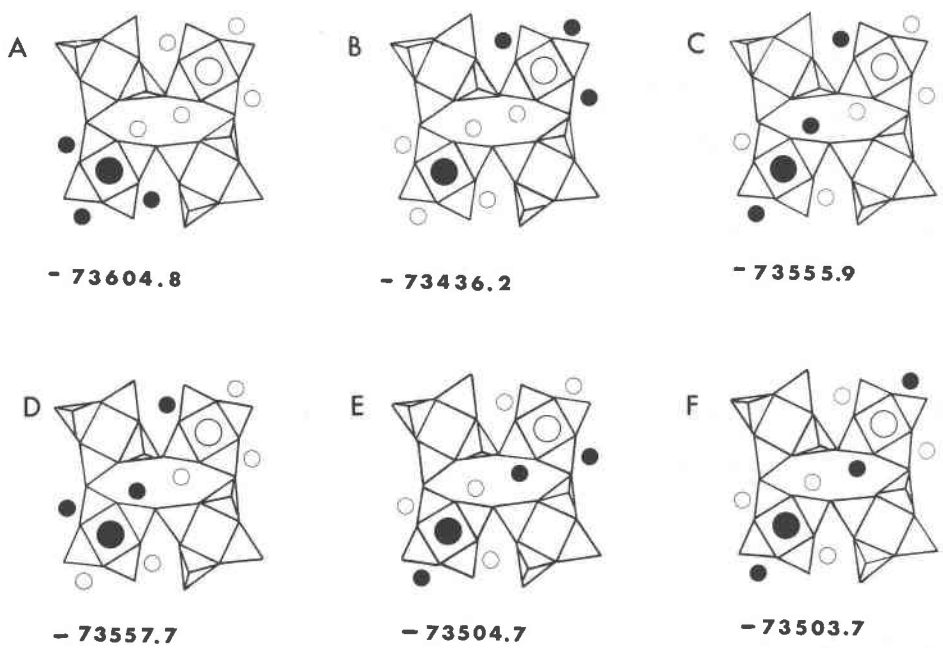

Fig. 3. Projection down c of an intermediate scapolite showing the different alkali configurations and their structure energies. Small solid circles represent calcium atoms, large solid circles represent carbonate radicals, small open circles represent sodium atoms, and large open circles represent chlorine atoms. Energies are in kcal/mole.

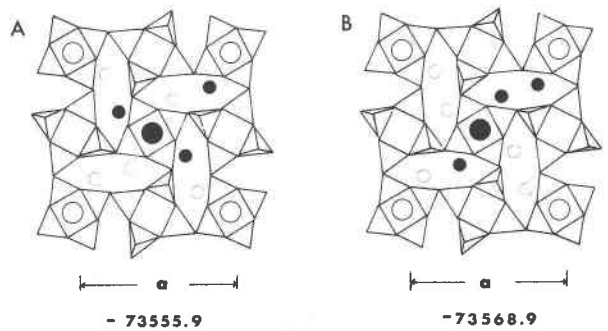

Fig. 4. Projection down c of an intermediate scapolite showing the types of shared channels possible using the configuration shown in Fig. 3C. Electrostatic energies in kcal/mole are given for each possibility. Symbols for the atoms are the same as in Fig. 3.

disordered. To reproduce this disorder in the calculations would require using at least four unit cells, involving large amounts of computer time. Instead, we have performed all of our calculations using one of the CO_3^{2-} positions reported by Levien and Papike (1976). Test calculations show insignificant differences in the total structure energy for models using the alternate CO_3^{2-} positions reported by Levien and Papike (1976). Second, we assumed that the distance of the Ca^{2+} and Na^+ cations from Cl^- and CO_3^{2-} anions remains unchanged in the various models. This assumption derives from our use of structure refinement data (Levien and Papike, 1976) that assumes Ca^{2+} and Na^+ are equidistant from Cl^- and CO_3^{2-}. However, because the oval-shaped cavities occupied by Ca^{2+} and Na^+ are large, the distances between alkali cations and Cl^- and CO_3^{2-} probably do change with changing configurations. Our calculations show, however, that the adjustments in alkali positions with changing configurations are small and account for less than 5 kcal/mole in the total energy. Third, throughout our calculations we have assumed that the frame work remains unchanged. Resulting energy differences are due, therefore, only to different configurations of alkali cations, Cl^-, and CO_3^{2-}.

Results

The six possible configurations of Na^+ and Ca^{2+} around Cl^- and CO_3^{2-} and their corresponding energies are shown in Figures 3A through 3F. Structure energy values are given per unit cell of scapolite. The most energetically favorable configuration places the maximum number of Na^+ around Cl^- and the maximum number of Ca^{2+} around CO_3^{2-}. The structure energy increases as more Na^+ is placed around CO_3^{2-}, and Ca^{2+} around Cl^-. The energy maximum occurs when Ca^{2+} surrounds Cl^- to the extent possible, and Na^+ surrounds CO_3^{2-}. The energy differences between this structure (Fig. 3B) and the most favorable structure (Fig. 3A) is approximately 215 kcal/mole. These energy calculations, therefore, demonstrate that there is a preference for Na^+ to surround Cl^- and Ca^{2+} to surround CO_3^{2-} in scapolite.

It is also possible that there are favorable combinations of Na^+ and Ca^{2+} distributions within the oval-shaped cavities in scapolite. To test this possibility, we calculated electrostatic energies for the two different possibilities of channel sharing with the configurations shown in Figure 3C. One possibility results in Na–Na and Na–Ca shared channels (Fig. 4A) and the other possibility gives Na–Na, Ca–Ca, and Na–Ca shared channels (Fig. 4B). The energy difference between these two possibilities is not significant (approximately 13 kcal/mole), probably because adjacent alkali cations in the channels are separated by about 4.9Å.

Using the program WMIN (Busing, 1981) we also calculated the minimum energy positions of Na^+ and Ca^{2+} surrounding Cl^- and CO_3^{2-} for the four different CO_3^{2-} configurations reported by Levien and Papike (1976). During the minimizations, only the Na^+ or Ca^{2+} positional parameters were allowed to vary. The position of Ca^{2+} changes slightly (a maximum difference of 0.26Å between Ca^{2+} positions) for different CO_3^{2-} configurations, with Ca^{2+} shifting toward the nearest carbonate oxygen. This positional disorder is partly responsible for the relatively large anisotropic temperature factor determined for the Na^+,Ca^{2+} site by Levien and Papike (1976). The minimized distances for Na–Cl and Ca–O (CO_3^{2-}) are 3.16Å and 3.34Å, respectively. The similarity of these distances accounts for the difficulty Levien and Papike (1976) report in resolving two distinct sites for Na^+ and Ca^{2+}.

Table 1. Short range energy parameters used in the electrostatic energy calculations (from Post and Burnham, in prep.)*

Ion Pair	λ (kcal/mole)	ρ (Å)
Si-O	85604	0.2428
Al-O	79447	0.2461
Na-O	134608	0.2387
Ca-O	160461	0.2516
C-O	47777	0.2376
Si-Cl	68701	0.2853
Al-Cl	70818	0.2831
Na-Cl	103596	0.2727
Ca-Cl	189745	0.2729
C-Cl	47140	0.2752
O-O	69551	0.2876
O-Cl	84097	0.2948
Cl-Cl	66233	0.3173

*Shell radius for O^{2-} = 1.01Å and for Cl^- = 1.64Å

Antiphase domains in scapolite

Antiphase domains have been observed in several scapolite specimens (Phakey and Ghose, 1972; Buseck and Iijima, 1974; Oterdoom and Wenk, 1983), indicating short range ordering. Phakey and Ghose (1972) interpret the antiphase domains as due to ordering of Cl^- and CO_3^{2-} in scapolite. Although antiphase domains seen by Oterdoom and Wenk (1983) have a similar morphology to those observed by Phakey and Ghose (1972), they are interpreted as arising from Al^{3+} and Si^{4+} ordering between T2 and T3 sites, since their scapolite contains very little Cl^-.

We have used energy calculations to investigate whether it is energetically favorable for Cl^- and CO_3^{2-} (or more appropriately, Na_4Cl and Ca_4CO_3 clusters) to order in scapolite, and therefore possibly create antiphase domains. Calculations were performed on a supercell consisting of four normal scapolite unit cells that was constructed by doubling the lengths of the **a** and **b** axes. Structure energies were calculated for several different arrangements of Na_4Cl and Ca_4CO_3 clusters within the supercell (Figs. 5 and 6). Our calculations indicate that the most energetically favorable arrangement is when Na_4Cl and Ca_4CO_3 have the same configuration in each subcell, representing the fully ordered case (Fig. 5A). All of the remaining models represented in Figure 5 (B–D) and Figure 6 are energetically less favorable than the fully ordered case. Therefore, arguments based entirely on structure energetics suggest that a driving force for ordering of Na_4Cl and Ca_4CO_3 exists in scapolite, and consequently observed antiphase domains could result from ordering these species.

These results do not preclude the possibility of domains arising from short-range ordering of Al^{3+} and Si^{4+} within the tetrahedral framework, as suggested by Oterdoom and Wenk (1983), or the possibility that Na_4Cl and Ca_4CO_3 ordering is coupled to short-range ordering of Al^{3+} and Si^{4+}. Our results do, however, suggest an impetus for the formation of antiphase domains above and beyond, and not necessarily coupled to, Al^{3+} and Si^{4+} ordering. In fact, both types of antiphase domains may exist in scapolite.

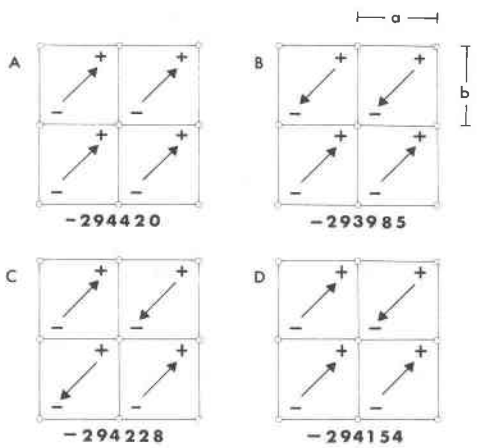

Fig. 5. Simplified diagram of 4 cells of scapolite projected down **c**. Arrows point along (111) from CO_3^{2-} to Cl^-. Plus represents the position 3/4,3/4,3/4, and minus represents the position 1/4,1/4,1/4. Energies are in kcal/mole.

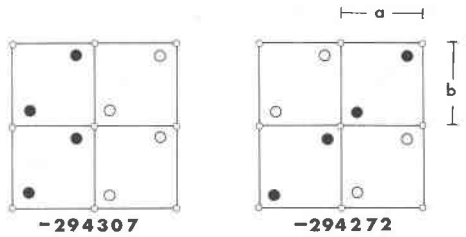

Fig. 6. Simplified diagram of 4 cells of scapolite projected down **c**. Large solid circles represent carbonate-calcium clusters, and large open circles represent chlorine-sodium clusters.

Scapolite stoichiometry

Three exchange reactions are possible in scapolites: $NaCl\overline{CaCO_3}$, $NaSi\overline{CaAl}$, and $AlCO_3\overline{SiCl}$. There is evidence, however, that none of these reactions behaves independently (Papike, 1964; Evans et al., 1969). Based on microprobe analyses, these authors suggested that for scapolite with Ca/(Ca+Na) less than 0.75, the composition varies by the combined reaction $Na_2SiCl\overline{Ca_2AlCO_3}$; but when Ca/(Ca+Na) is greater than 0.75, the composition varies by the reaction $NaSi\overline{CaAl}$. As yet, there is no adequate explanation for this peculiar substitution scheme.

Lin (1975) argued that the unusual compositional variations are due to gross differences in behavior of Cl^- and CO_3^{2-} in the crystal structure. According to this interpretation, substitution of Cl^- and CO_3^{2-} causes tilting of the planar carbonate group, displacement of Ca^{2+} and Na^+ atoms along the **c** axis, and ordering of Al^{3+} and Si^{4+}. The compositional variations are explained (Lin, 1975) in terms of local neutralization of electrostatic valences between the tilted carbonate group, the displaced Na^+ and Ca^{2+} ions, and the tetrahedral framework. However, tilting of the carbonate group and displacement of Na^+ and Ca^{2+} along the **c** axis, central to Lin's (1975) argument, have not been confirmed in crystal structure refinements of intermediate scapolites (Levien and Papike, 1976; Papike and Stephenson, 1966). We now present evidence suggesting that the compositional variations observed in scapolite are simply the result of achieving local charge balance between Na^+ and Ca^{2+} cations and Cl^- and CO_3^{2-} anions.

We plot Al/(Al+Si) versus Ca/(Ca+Na) and Al/(Al+Si) versus Cl^- for published scapolite analyses in Figures 7 and 8. The upper and lower bounding lines shown in Figure 7 represent the maximum Ca^{2+} and Na^+ content,

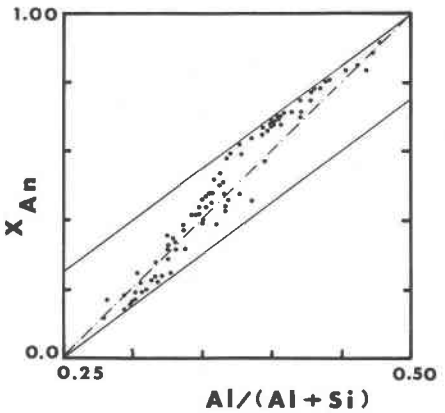

Fig. 7. Al/(Al+Si) versus Ca/(Ca+Na) = X_{An} for scapolites. The upper bounding line represents pure carbonate members, and the lower bounding line represents pure chlorine members. The dash–dot line represents the scapolite compositions where there is local charge balance on chlorine and carbonate sites. Scapolite analyses are from Peterson et al. (1979), Lovering and White (1964, 1969), Llambías et al. (1977), Shaw (1960), Shay (1975), Evans et al. (1969), Vanko and Bishop (1982), Aitken (1983), Cook (1974), and Graziani and Lucchesi (1982).

respectively, for a scapolite with a given Al/(Al+Si) ratio. For example, a scapolite with Al/(Al+Si) of 1/3 would have Ca/(Ca+Na) = 0.5 (upper bounding line) if it were a pure carbonate member, or Ca/(Ca+Na) = 0.25 (lower bounding line) if it were a pure chlorine member. Variations of Ca/(Ca+Na) between 0.25 and 0.5 at this Al/(Al+Si) ratio occur through the substitution $NaCl\overline{CaCO_3}$. Varying the composition of scapolite by the reaction $NaCl\overline{CaCO_3}$, therefore, causes displacements vertically in Figure 7, and varying composition by the reaction $NaSi\overline{CaAl}$ causes displacements parallel to the bounding lines. The observed compositional distribution shown in Figures 7 and 8 is the same as that observed by Papike (1964) and Evans et al. (1969), supporting the suggestion that the substitution schemes in scapolite do not behave independently.

Calculations

We have calculated local charge balance for the Cl^-, CO_3^{2-} site for a variety of scapolite compositions. At any given Al/(Al+Si) ratio, there is a range of theoretically possible compositions; within this range both overbonding and underbonding situations must exist between the alkali cations and the Cl^-, CO_3^{2-}. There is, however, only one unique Ca/(Ca+Na) ratio, for a given Al/(Al+Si) ratio, for which exact local charge balance exists between Na^+, Ca^{2+} and Cl^-, CO_3^{2-}. This unique ratio changes as the Al/(Al+Si) ratio changes because of the coupling $NaSi\overline{CaAl}$.

The algorithm for calculating the deviation from electrical neutrality on the anion site is as follows:

$$((A+X)\ 2/4) + ((B+Y)\ 1/4) + (-2)\ X + (-1)\ Y = \Delta \quad (1)$$

where X = mole fraction CO_3^{2-} = $(CO_3/(CO_3+Cl))$, Y = mole fraction Cl^-, A = the number of Ca^{2+} cations balanced by Al^{3+} in the framework, B = the number of Na^+ cations balanced by Si^{4+} in the framework, and Δ is the deviation from electrical neutrality. The +2, +1, −1, and −2 are the charges on the calcium, sodium, chlorine, and the carbonate radical, respectively. Our calculations are based on the assumption that the Cl^- and CO^{2-} are coordinated to four alkali ions. We do not consider the coordination of alkalis by oxygens in these calculations. Division by 4 is necessary because each anion/radical sees only 1/4 of the total alkali charge. The other 3/4 of the alkali charge belongs to the framework, as a result of the scapolite stoichiometry. As an example, for composition $Ca_3Al_6Si_6O_{24}CaCO_3$, equation (1) becomes:

$$((3+X)\ 1/2) + (O+Y)\ 1/4 + (-2)\ X + (-1)\ Y = \Delta$$

In this case $\Delta = 0$, and local charge balance is obtained. Using this equation, Δ can be calculated for various fractions of CO_3^{2-} and Cl^- on the anion sites.

Results

Figure 9 shows the accessible scapolite chemical composition space contoured for Δ. The zero line passes through those compositions for which the anion site has complete local charge balance. For example, scapolite with Al/(Al+Si) = 0.5 must contain all Ca^{2+} cations and CO_3^{2-} radicals to obtain a charge-balanced anion site. Substitution of NaCl for $CaCO_3$ results in underbonding on the anion site. Similarly, scapolite with Al/(Al+Si) = 0.375 requires equal amounts of Cl^- and CO_3^{2-} (Ca/(Ca+Na) = 0.5) for charge balance on the anion site. More chlorine-rich compositions for this Al/(Al+Si) ratio are overbonded, whereas more carbonate-rich compositions are underbonded.

Of particular interest is the similarity of the $\Delta = 0.0$

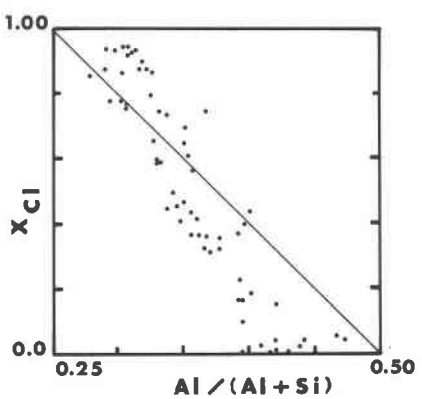

Fig. 8. Al/(Al+Si) versus X_{Cl} for scapolites. X_{Cl} is Cl/(Cl+CO_3). The solid line represents the scapolite composition where there is local charge balance on the chlorine and carbonate sites. Scapolite analyses are from the same references given in Fig. 7.

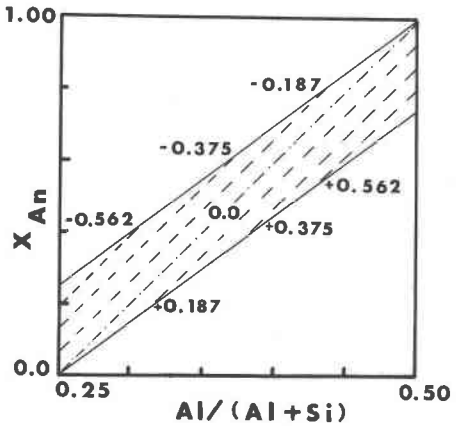

Fig. 9. Contours of local charge balance on the chlorine and carbonate sites for Al/(Al+Si) versus X_{An} = Ca/(Ca+Na) in scapolites. Positive numbers represent overbonding situations and negative numbers represent underbonding situations on the large anion sites.

contour of Figure 9 with the observed compositional trend shown in Figure 7. Having already noted that the substitution schemes in scapolite do not behave independently, we suggest further that local charge balance on the alkali site is the controlling factor responsible for the composition path observed for the marialite-meionite series.

Although the actual composition of a scapolite in a chemical system will be determined by the saturating phases, the composition will, in part, also be determined by the degree of curvature of the Gibbs free energy surface of scapolite itself within its composition space. This curvature is dependent on the energetics of the structure and is independent of the saturating phases. Our calculations are only an approximation to the true energetics of the anion site and the framework, but as a first order approximation we feel the trends they exhibit are valid. We suggest, therefore, that the unfavorable bonding situations are energetically unfavorable for the scapolite structure as a whole and will be manifested as strong curvature on the Gibbs free energy surface of scapolite. Assuming, then, that unfavorable bonding situations are the most important contributing factor to the shape of the Gibbs free energy surface of scapolite, the strongest curvature of this surface must be normal to the $\Delta = 0.0$ line (Fig. 9). Higher-order terms in the energetics will result in small irregularities in the Gibbs free energy surface. In our interpretation, deviations from the $\Delta = 0.0$ line are due primarily to the positions of the Gibbs free energy surfaces of saturating phases relative to that of scapolite, as well as to higher-order terms not considered in our calculations.

Conclusions

Three conclusions emerge from this study. First, energy calculations show that Na^+ should favor positions adjacent to Cl^-, and Ca^{2+} is most favorably situated around CO_3^{2-}. Second, our calculations suggest that antiphase domains may arise from short-range ordering of Na_4Cl and Ca_4CO_3 clusters in scapolite. This ordering will be the greatest when there are equal amounts of Cl^- and CO_3^{2-} in the structure. It is also possible that short-range ordering of Al^{3+} and Si^{4+} can occur, creating more than one type of antiphase domain. Third, the unusual compositional variations observed in the marialite–meionite series may be the result of crystallographic constraints on the two independent exchange reactions $NaCl\overline{CaCO_3}$ and $NaSi\overline{CaAl}$. Based on the similarity of the composition path of naturally occurring scapolite and the theoretical composition of scapolite representing local charge balance on the anion site, we suggest that charge balance between alkali cations (Ca^{2+}, Na^+) and the Cl^- and CO_3^{2-} anions is the controlling factor governing the compositions of scapolites.

Acknowledgments

This work was funded by NSF grants EAR 79-20095 to Charles W. Burnham and EAR 81-15686 to James B. Thompson, Jr. We appreciate the reviews of J. J. Papike, G. V. Gibbs, and D. R. Veblen from which this manuscript has benefited greatly. We thank J. B. Thompson, Jr., for his helpful comments.

References

Aitken, B. G. (1983) T–X_{CO_2} stability relations and phase equilibria of a calcic carbonate scapolite. Geochimica et Cosmochimica Acta, 47, 351–362.

Buseck, P. R. and Iijima, Sumio (1974) High resolution electron microscopy of silicates. American Mineralogist, 59, 1–21.

Busing, W. R. (1981) Oak Ridge National Laboratory Spec. Pub. 5747, Oak Ridge, Tennessee.

Cook, L. P. (1974) Metamorphic rocks of the Nashoba Formation, eastern Massachusetts. Ph.D. Thesis, Harvard University, Cambridge.

Evans, D. W., Shaw, D. M., and Haughton, D. R. (1969) Scapolite stoichiometry. Contributions to Mineralogy and Petrology, 245, 293–305.

Gordon, R. G. and Kim, Y. S. (1972) Theory of the forces between closed shell atoms and molecules. Journal of Chemical Physics, 6, 3122–3133.

Graziani, Giorgio and Lucchesi, Sergio (1982) The thermal behavior of scapolites. American Mineralogist, 67, 1229–1241.

Kittel, Charles (1976) Introduction to Solid State Physics, 5th ed. Wiley, New York.

Levien, Louise and Papike, J. J. (1976) Scapolite crystal chemistry: aluminum-silicon distributions, carbonate disorder, and thermal expansion. American Mineralogist, 61, 864–877.

Lin, S. B. (1975) Crystal chemistry and stoichiometry of the scapolite group. Acta Geologica Taiwanica, 18, 36–48.

Lin, S. B. and Burley, B. J. (1973a) Crystal structure of a sodium and chlorine-rich scapolite. Acta Crystallographica, B29, 1272–1278.

Lin, S. B. and Burley, B. J. (1973b) The crystal structure of meionite. Acta Crystallographica, B29, 2024–2026.

Lin, S. B. and Burley, B. J. (1975) The crystal structure of an intermediate scapolite-Wernerite. Acta Crystallographica, B31, 1806–1814.

Llambías, E. J., Gordillo, C. E., and Bedlioy, Dora (1977) Scapolite veins in a quartz monzodiorite stock from Los Molles, Mendoza, Argentina. American Mineralogist, 62, 132–135.

Lovering, J. F. and White, A. J. R. (1964) The significance of primary scapolite in granulitic inclusions from deep-seated pipes. Journal of Petrology, 5, 195–218.

Lovering, J. F. and White, A. J. R. (1969) Granulitic and eclogitic inclusions from basic pipes at Delegate. Australia. Contributions to Mineralogy and Petrology, 49, 4. o2.

Muhlhausen, C. W. and Gordon, R. G. (1981) Electron-gas theory of ionic crystals, including many-body effects. Physical Review B, 23, 900–923.

Oterdoom, W. H. and Wenk, H. R. (1983) Ordering and composition of scapolite: field observations and structural implications. Contributions to Mineralogy and Petrology, 83, 330–341.

Papike, J. J. (1964) The crystal structure and crystal chemistry of scapolite. Ph.D. Thesis, University of Minnesota.

Papike, J. J. and Zoltai, Tibor (1965) The crystal structure of a marialite scapolite. American Mineralogist, 50, 641–655.

Papike, J. J. and Stephenson, N. C. (1966) The crystal structure of mizzonite, a calcium and carbonate rich scapolite. American Mineralogist, 51, 1014–1027.

Peterson, R. C., Donnay, Gabrielle, and LePage, Yvon (1979) Sulfate disorder in scapolite. Canadian Mineralogist. 17, 53–61.

Phakey, P. P. and Ghose, Subrata (1972) Scapolite: observation of antiphase domain structure. Nature Physical Science, 238, 78–80.

Shay, Kenneth (1975) Mineralogic zoning in a scapolite-bearing skarn body on San Gorgonio Mountain, California. American Mineralogist, 60, 785–797.

Shaw, D. M. (1960) The geochemistry of scapolite. Part I. Previous work and general mineralogy. Journal of Petrology, 1, 218–260.

Thompson, J. B., Jr. (1982) Composition space: an algebraic and geometric approach. In J. M. Ferry, Ed., Reviews in Mineralogy, 10, 1–31. Mineralogical Society of America, Washington, D. C.

Vanko, D. A. and Bishop, F. C. (1982) Occurrence and origin of marialitic scapolite in the Humboldt lopolith, N. W. Nevada. Contributions to Mineralogy and Petrology, 81, 277–289.

Manuscript received, August 16, 1983;
accepted for publication, September 18, 1984.